symmetry

MDPI

Article

Holistic Symmetry Assessment Using Pedobarography after Treatment of Pertrochanteric Fractures in Elderly Patients

Karolina Gawronska [1,*] and Jacek Lorkowski [2,*]

[1] Rehabilitation Centre of the Central Clinical Hospital of the Ministry of the Internal Affairs and Administration, 137 Woloska Street, 02-507 Warsaw, Poland
[2] Clinical Department of Orthopaedics, Traumatology and Sports of the Central Clinical Hospital of the Ministry of the Internal Affairs and Administration, 137 Woloska Street, 02-507 Warsaw, Poland
* Correspondence: kegawronska@gmail.com (K.G.); jacek.lorkowski@gmail.com (J.L.); Tel.: +48-518958043 (K.G.); +48-606452887 (J.L.)

Abstract: Pertrochanteric fractures (PFs) are life threatening due to the prolonged immobilization of the elderly patient that affects, indirectly, the function of most organs. PFs may have an impact on the symmetry of the human body and contribute to poor global alignment. The aim of the study is to evaluate the functional, pedobarographic and radiological outcomes in a group of subjects with PFs treated with either a dynamic hip screw (DHS) or an intramedullary gamma nail fixation. A study group of 40 patients, admitted to hospital for pertrochanteric fractures between 2015 and 2019, at a mean age of 74.87 (range 65–99), were enrolled. A control group included 20 subjects free from significant disorders of the musculoskeletal system and any other disorders that might induce a compensatory abnormal gait pattern. Functional results were assessed by the Harris Hip Score, and the plantar pressure distribution and arch index were measured with a pedobarographic examination. Radiographic parameters were assessed based on the preoperative and postoperative standing AP pelvic radiographs and axial projection of the hip. The obtained results were evaluated at 9-month follow-up. The obtained results showed no significant difference between both study groups within the scope of the variables under study. To sum up, surgical treatment, either with DHS or intramedullary gamma nail fixation, and rehabilitation treatment support the symmetry of the musculoskeletal system. However, the full return of symmetry was not achieved at 9-month follow-up compared to the control group.

Keywords: hip fractures; elderly; pedobarography; alignment; osteosynthesis; dynamic hip screw; intramedullary gamma nail

check for updates

Citation: Gawronska, K.; Lorkowski, J. Holistic Symmetry Assessment Using Pedobarography after Treatment of Pertrochanteric Fractures in Elderly Patients. *Symmetry* **2022**, *14*, 1798. https://doi.org/10.3390/sym14091798

Academic Editors: John H. Graham and Chris Bishop

Received: 30 July 2022
Accepted: 25 August 2022
Published: 30 August 2022

Publisher's Note: MDPI stays neutral with regard to jurisdictional claims in published maps and institutional affiliations.

Copyright: © 2022 by the authors. Licensee MDPI, Basel, Switzerland. This article is an open access article distributed under the terms and conditions of the Creative Commons Attribution (CC BY) license (https://creativecommons.org/licenses/by/4.0/).

1. Introduction

The history of science has shown that whatever was important has repeatedly seemed to have already been discovered. That was also the case before the discovery of the constitute elements of an atom, quantum mechanics or quarks. However, this also applies to ratios found in geometry, which actually exist in the broadly understood nature on both the macro- and micro-scales. The golden number φ is the ratio well known for centuries but constantly re-discovered. Although fractals were previously partially known, it was not until 1983 that they were defined by Benoît B. Mandelbrot in "The Fractal Geometry of Nature" [1]. This is also the case with symmetry. Symmetry is omnipresent. In Greek philosophy, symmetry acquired a meaning based on a relation of ideal proportions expressed in natural numbers. That relation fulfilled the fundamental function of harmonizing different elements into a cohesive whole. In this manner, symmetry has become one of the key elements to describe the idea of harmony, beauty and unity [2]. The beauty canons known from Ancient Greece and then the period of Renaissance were grounded on symmetry and the "golden proportion" expressed as φ. The axial symmetry of the human body does not represent absolute symmetry, as evidenced by sculptures by Phidias or paintings by Leonardo da Vinci. We continue to learn what percentage of asymmetry is normal and what is pathological. It significantly depends on the dominance of one or the other limb, the type of sport practiced or profession performed over the years. The symmetry of the human body changes with age [3]. The age-related involution changes observed in all human systems, including particularly the musculoskeletal one, usually remain in a coherent relationship with one another. This concept, described by Immanuel Kant, in terms of involutional changes in the musculoskeletal system covers both micro and macro changes. These primarily include osteoporosis defined as a reduction in bone tissue density; therefore, the loss of its mass, joint degeneration, and the loss of muscle mass and strength [4]. All these cause disturbances in the proportions of the human body.

The changes in the symmetry of the human body in the older population are best observed by looking at the postural changes in the spine, such as thoracic hyperkyphosis (Dowager's Hump) or lumbar kyphosis. Such changes lead to an increased deflection of the body's centre of gravity, which can contribute to imbalances and therefore may contribute to falls and fractures in the elderly. The biomechanical properties of the skeleton reduce its strength and contribute to poor sagittal alignment [5,6]. Moreover, visual field and visual quality impairment affect postural control. The analysis of the literature indicates that the main age-related eye diseases such as glaucoma, macular degeneration, cataracts, weakness in contrast and depth vision and accommodation disorders, as well as limited visual motion perception, cause, for example, the excessive tilt of a torso and the tilt of the head to one side, which additionally interfere with body symmetry and increase the risk of falls [7]. It is estimated that 87% of fractures in the 65+ age group are caused by falls. Fractures of the tibia and fibula (20.5%), ribs and sternum (19.1%) and the proximal femur (18.9%) are the most common injures. Fractures of the proximal end of the femur, including femoral neck and pertrochanteric fractures (PFs), are particularly life threatening due to the immobilization of the elderly patient [8]. It should be remembered that various physiological processes are additionally influenced by the pleiotropic effects of medications. Efforts are taken to slow down certain processes, such as the development of osteoporosis. It is a commonly recognized fact though that, for example, bisphosphonates used in the treatment of osteoporosis are considered to be one of the causes of transverse pathological femoral shaft fractures.

The standard in the treatment of PFs is surgery. Dynamic hip screws (DHS), trochanteric gamma nails and reconstruction nails are most commonly used for anastomoses [9–11]. The selection of the appropriate fixation system depends on the type of fracture and the operator's experience and may vary in different medical centers [12]. The large number of complications and poor outcomes after PFs' treatment is widely known and reported in the literature. The treatment process often does not include compensatory mechanisms, without which results cannot be assessed in a holistic manner. One of the indirect methods, but often very sensitive, is pedobarography. However, as shown by the literature review and our own observations, the use of this method across the world is negligible in the case of treatment after a fracture of the proximal end of the femur. Pedobarographic examination is particularly useful in the diagnosis and rehabilitation of the foot after the surgical treatment of pertrochanteric fractures. It is a non-invasive diagnostic method of the locomotor system based on the plantar pressure distribution. The analysis provides information about its size and distribution along with a graphic representation of the possible asymmetry, pathological overloads or lack of pressure [13]. The popularization of the measurement of symmetry in plantar pressure distribution based on pedobarography may allow for the multi-disciplinary prevention of falls and better treatment results of PFs.

The aim of this study is to assess the functional, pedobarographic and radiological outcomes in a group of patients with pertrochanteric fractures treated with either DHS or intramedullary gamma nail fixation, and particularly to:

- quantify and draw inferences on observed differences in functional status.
- quantify and draw inferences on observed differences in the symmetry of pedobarographic assessment.
- quantify and draw inferences on observed differences in the assessment of symmetry in selected parameters based on the X-rays.

2. Materials and Methods

2.1. Subjects

Forty patients (33 women, 7 men), admitted to hospital for pertrochanteric fractures between 2015 and 2019, at a mean age of 74.87 (range 65–99), participated in the study, as shown in Table 1. The study group was divided into a subgroup of patients treated with DHS screw plate (20 patients) and patients who underwent surgery using an intramedullary Gamma nail (20 patients). One patient from DHS group pointed to the left upper limb as dominant, the remaining subjects indicated the right upper limb as dominant (right-handed). Control group at a mean age of 71.55 (range 65–82) consisted of 20 subjects (11 women, 9 men). None of the control group reported any current pain; they were free of significant disorders of the musculoskeletal system: joint disorders and lower limb disease, and any other neuromuscular or chromosomal disorders, as well as of systemic diseases that may cause a compensatory abnormal gait pattern. All subjects pointed to the right upper limb as dominant.

Table 1. Demographic characteristics.

	DHS Group (n = 20)	Gamma Group (n = 20)	Control Group (n = 20)
Age	73.80 ± 8.95	75.95 ± 8.88	71.55 ± 5.41
Body mass, kg	73.75 ± 13.07	73.65 ± 15.04	83.65 ± 13.12
Body high, cm	168.95 ± 10.17	166.70 ± 9.10	170.60 ± 9.76
BMI	25.72 ± 3.06	26.27 ± 3.47	28.74 ± 2.95

Values are expressed as means ± standard deviation.

Each person involved in the study gave informed consent for inclusion before participating in the study. The study was conducted in accordance with the Declaration of Helsinki, and the protocol was approved by the Ethics Committee of the Central Clinical Hospital of the Ministry of the Internal Affairs and Administration in Warsaw—32.2019.

2.2. Inclusion Criteria

- Patients admitted for a hospital stay in the department of orthopedics and traumatology of the motor organ in the period from 1 January 2015 to 31 December 2019 with the primary diagnosis of pertrochanteric fracture;
- patients who underwent fixation of pertrochanteric fracture, performed by one/the same operator (operating surgeon—consultant);
- type of fixation used: DHS screw plate or intramedullary Gamma nail;
- type of fracture according to AO classification—A1, A2, A3;
- aged 65+;
- a minimum postoperative follow-up of 9 months

2.3. Exclusion Criteria

- Patients who had a poor outcome due to comorbidities, who did not report to outpatient control;
- a different type of fracture fixation was used;
- multi-site musculoskeletal injuries;
- pathological fracture (excluding osteoporosis).

2.4. Data Analysis

Clinical outcome was assessed using the Harris Hip Score (HHS) preceded by a physical examination of the musculoskeletal system in the form of linear measurements (length and circumference of the lower limbs), examination of the range of motion of lower extremity joints, assessment of lower limb muscle strength, and assessment of muscle contractures [14]. The HHS scale was developed for the assessment of the results of hip surgery, and is intended to evaluate various hip disabilities and methods of treatment in an adult population, including functional outcome after pertrochanteric hip fracture [15–17]. The scale applied in the study consists of 10 items covering domains of pain, function, functional activities, deformity and hip range of motion. The interpretation of outcome using the modified Harris hip score was as follows: <70 (poor result), 70–79 (fair result), 80–89 (good result) and >90 (excellent result). Clinical assessment was performed during follow-up visit as part of an outpatient treatment 9 months after the surgery.

Pedobarographic Assessment

Pedobarographic examination was carried out in the static mode with device calibration before each patient, using the pressure platform (EPS/R2, Loran Engineering, Bologne, Italy). The platform contains a total of 2096 pressure sensors of 1 cm^2 distributed in an area of 48 cm × 48 cm. The range of pressure was 30–400 kPa, and acquisition frequency 100 Hz. Before the examination, the patient's plantar foot was masked into regions. Subjects were supposed to maintain an upright position and barefoot. The instructions given to the patients also concerned keeping their bodies symmetrical and looking straight ahead during the assessment. The main examination was preceded by a trial test aimed at familiarizing participants with the equipment and procedure of the test. The test room was arranged with the platform in a central position at an equal distance from the left and right wall in relation to the subject and minimum 5 m to the front wall in order to achieve a symmetrical view. The entire test room was of a uniform color, without the impression of a one-sided narrowing or expanding of the space. The actual testing was continued until the most common three reproducible results were obtained. Duration of each individual study was 5 s, but the median duration of the overall study including instruction for subjects, trial test, actual test and short rest between trials was 10 min [18]. Data acquisition was performed using Biomech 4.0 software (Loran Engineering, Italy). The study was based on foot classification according to Cavanagh. Following regions were distinguished T1 (Hallux), Toes 2–5, M1–M5 (area under the 1st–5th metatarsal head), MF (midfoot), MH (medial heel), LH (lateral heel) [6]. The following parameters were obtained: measurement of plantar pressure distribution (average and maximum values measured in kilopascal—Kpa) during standing, entire support area for each foot (%), distribution of maximum and average pressures on individual foot regions according to the Cavanagh model and assessment of the foot arch during standing (AI—arch index) according to Rogers-Cavanagh [19,20].

Radiographic Analysis

Radiographic analysis was performed on the basis of the preoperative and postoperative standing, AP pelvic X-ray images and axial projection of the hip at 9-month observation. Radiographs were assessed for:

- fracture union (full union vs. non-union present);
- neck-shaft angle (NSA)—operated femur and its opposite side (assessment for the presence of valgus or varus position);
- the position of the neck screw in relation to the axis of the femoral neck (screw located on the axis or below the axis vs. located above the axis);
- the axis of the intramedullary nail in relation to the axis of the femur (evaluated in the anterior–posterior view: varus position—the distal part of the nail resting on the medial cortex; axial position—the own axis of the nail coincides with the axis of the femoral shaft; valgus position—the distal part of the nail resting on the cortex layer of the femur on the lateral side);

- the minimum distance between the tip of the neck screw and the articular surface of the femoral head (arithmetic mean of the distance measured in the anterior–posterior and axial projection);
- shortened length of the operated limb (the difference in the height of the lesser trochanter position) by >1 cm.

2.5. Statistical Analysis

Statistical analyses were performed with Statistical software—Statistica 10.0 working on Windows 10 (StatSoft, Cracow, Poland). The data were normally distributed, as tested by the *t*-test for independent sample tests. Data with a distribution inconsistent with the normal (plantar pressure distribution in masked regions of the foot) were analyzed with the Mann–Whitney U Test. The level of statistical significance was set at $p < 0.05$ for all analyses.

3. Results

3.1. Functional Outcomes

Comparing functional outcomes assessed using the Harris Hip Score in Table 2, there is no difference between the two groups (DHS Group vs. Gamma Group) at 9–12 months follow-up. Functional symmetry was maintained between the two study groups.

Table 2. Comparison of outcomes using Harris Hip Score in DHS group (n = 20) and gamma group (n = 20).

	DHS Group	Gamma Group	*p*
Harris Hip Score	80.16 ± 5.00	81.80 ± 2.96	0.21

Values are expressed as mean ± standard deviation.

The mean outcome for control group is 92.65 ± 4.22.

3.2. Pedobarography

Table 3 shows the comparison of the plantar pressure distribution between the operated and non-operated side in the DHS group and gamma group (the entire foot surface). The obtained results do not indicate any significant difference in the loading of the operated and non-operated side. Foot loading between the operated and non-operated lower limb is symmetrical.

Table 3. Comparison of the plantar pressure distribution of the entire foot in operated vs. non-operated side in DHS group (n = 20) and gamma group (n = 20); mean pressure values in Kpa.

	Operated Side	Opposite Side	*p*
Entire foot loading—DHS	58.74 ± 10.14	59.21 ± 10.32	0.88
Entire foot loading—Gamma	56.58 ± 10.06	57.45 ± 9.99	0.78

Values are expressed as mean ± standard deviation.

In Table 4, the plantar pressure distribution between the left and right foot in the control group (the entire foot surface) is compared. The obtained results indicate symmetrical loading of the left and right foot.

Table 4. Comparison of the plantar pressure distribution of the entire left foot vs. right foot in control group (n = 20); mean pressure values in Kpa.

	Left Side	Right Side	*p*
Entire foot loading	64.35 ± 8.38	64.87 ± 8.93	0.85

Values are expressed as mean ± standard deviation.

Table 5 shows the comparison of the foot loading on the operated side in the DHS group with the foot loading on the operated side in the gamma group, as well as the foot loading of the non-operated side in the DHS group in relation to the foot loading of the non-operated side in the gamma group. The result shows the pressure mean values of the entire foot in Kpa. The obtained results do not indicate any significant difference in the loading of the DHS and gamma group; the symmetry between the study groups in terms of entire foot loading was maintained.

Table 5. Comparison of the plantar pressure distribution of the entire foot in operated and non-operated side in DHS group (n = 20) vs. gamma group (n = 20); mean pressure values in Kpa.

	DHS Group	Gamma Group	p
Entire foot loading operated side	58.74 ± 10.14	56.58 ± 10.06	0.50
Entire foot loading non-operated side	59.21 ± 10.32	57.45 ± 9.99	0.59

Values are expressed as mean ± standard deviation.

Table 6 shows the comparison of the entire foot pressure distribution between the DHS and control groups. The lower limb on the operated side was compared with the lower limb on the same side in the control group. The non-operated limb was compared by analogy. The obtained results indicate a significant difference in the foot loading on the opposite side, so we can say that symmetry was not preserved.

Table 6. Comparison of the plantar pressure distribution of the entire foot in operated and non-operated side in DHS group (n = 20) vs. control group (n = 20); mean pressure values in Kpa.

	DHS Group	Control Group	p
Entire foot loading operated side	58.74 ± 10.14	63.76 ± 9.08	0.10
Entire foot loading non-operated side	59.21 ± 10.32	65.46 ± 8.12	0.04 *

Values are expressed as mean ± standard deviation. * $p < 0.05$.

Table 7 shows the comparison of the entire foot pressure distribution between the gamma and control groups. The operated side was compared with the same side in the control group. The non-operated side was compared by analogy. The obtained results indicate a significant difference in the foot loading on both sides.

Table 7. Comparison of the plantar pressure distribution of the entire foot in operated and non-operated side in gamma group (n = 20) vs. control group (n = 20); mean pressure values in Kpa.

	Gamma Group	Control Group	p
Entire foot loading operated side	56.58 ± 10.06	65.22 ± 7.78	0.00 *
Entire foot loading non-operated side	57.45 ± 9.99	64.00 ± 9.41	0.03 *

Values are expressed as mean ± standard deviation. * $p < 0.05$.

Table 8 shows the comparison of the foot pressure distribution between the DHS and gamma groups in the masked regions of the foot. The results concern the foot on the side of the operated lower limb. In all tested regions, the obtained results do not indicate any significant difference in the loading. The observed differences between the study groups are so small and statistically insignificant that we can say that the symmetry was preserved.

Table 8. Comparison of the plantar pressure distribution in masked regions of the foot in DHS group (n = 20) vs. gamma group (n = 20). The result shows mean pressure values in Kpa on the operated side.

Masked Regions	DHS Group	Gamma Group	*p*
T1 (Hallux)	359.00	461.00	0.17
T2–5 (Toes 2–5)	367.50	452.50	0.25
M1 (1 Metatarsal head)	380.00	440.00	0.43
M2 (2 Metatarsal head)	428.00	392.00	0.64
M3 (3 Metatarsal head)	417.00	403.00	0.86
M4 (4 Metatarsal head)	395.50	424.50	0.7
M5 (5 Metatarsal head)	383.00	437.00	0.48
MF (Medial Foot)	412.00	408.00	0.97
MH (Medial Heel)	428.50	391.50	0.62
LH (Lateral Heel)	452.50	367.50	0.25

Values are expressed as rank sum.

Table 9 shows the comparison of the foot pressure distribution between the DHS and gamma groups in the masked regions of the foot. The results concern the foot on the side of the opposite lower limb. In all tested regions the obtained results do not indicate any significant difference in the loading.

Table 9. Comparison of the plantar pressure distribution in masked regions of the foot in DHS group (n = 20) vs. gamma group (n = 20). The result shows mean pressure values in Kpa on the opposite side.

Masked Regions	DHS Group	Gamma Group	*p*
T1 (Hallux)	425.50	394.50	0.68
T2–5 (Toes 2–5)	431.00	389.00	0.58
M1 (1 Metatarsal head)	389.50	430.50	0.58
M2 (2 Metatarsal head)	418.00	402.00	0.84
M3 (3 Metatarsal head)	405.50	414.50	0.9
M4 (4 Metatarsal head)	408.00	412.00	0.97
M5 (5 Metatarsal head)	421.00	399.00	0.78
MF (Medial Foot)	445.50	374.50	0.34
MH (Medial Heel)	465.50	354.50	0.13
LH (Lateral Heel)	451.00	369.00	0.28

Values are expressed as rank sum.

The following images (Figure 1A–C) show sample results of a pedobarographic examination of a man, 90 kg, treated with DHS (A); a man, 85 kg, treated with gamma nail (B); and a woman, 90 kg, from control group (C).

Comparing the arch index (Table 10) in both study groups, we notice a certain tendency. Different values were obtained in both cases. On the opposite side, the AI value is slightly higher than the AI in the operated foot, but it is not a statistically significant difference. The symmetry in the foot arch was preserved.

Table 10. Comparison of arch index of the operated side vs. opposite side in DHS group (n = 20) and gamma group (n = 20).

	Operated Side	Opposite Side	*p*
Arch Index DHS Group	26.69 ± 2.32	27.82 ± 3.84	0.26
Arch Index Gamma Group	25.42 ± 5.10	27.21 ± 4.94	0.27

Values are expressed as mean ± standard deviation.

In Table 11, higher values of the arch index were noted under the right foot, but the difference in the obtained values is not statistically significant.

Table 11. Comparison of arch index of left foot vs. right foot in the control group (n = 20).

	Left Side	Right Side	p
Arch Index Control Group	27.32 ± 3.99	28.02 ± 3.56	0.56

Values are expressed as mean ± standard deviation.

Table 12 shows the comparison of the arch index in the DHS group vs. the gamma group. The results refer to the operated and non-operated side.

Table 12. Comparison of the arch index of operated and non-operated side in DHS group (n = 20) vs. gamma group (n = 20).

	Gamma Group	Control Group	p
AI in operated limb	26.69 ± 2.32	25.42 ± 5.10	0.32
AI in opposite limb	27.59 ± 3.60	27.21 ± 4.93	0.78

Values are expressed as mean ± standard deviation.

Table 13 shows the comparison of the arch index between the DHS and control groups. The lower limb on the operated side was compared with the lower limb on the same side in the control group. The non-operated limb was compared by analogy. The obtained results indicate that the symmetry of the assessed parameter is maintained.

Table 13. Comparison of the arch index of operated and non-operated side in DHS group (n = 20) vs. control group (n = 20).

	DHS Group	Control Group	p
AI operated side	26.69 ± 2.32	27.57 ± 3.65	0.36
AI opposite side	27.82 ± 3.84	27.77 ± 3.94	0.97

Values are expressed as mean ± standard deviation.

Table 14 shows the comparison of the arch index between the gamma and control groups. The lower limb on the operated side was compared with the lower limb on the same side in the control group. The non-operated limb was compared by analogy. The obtained results do not indicate a significant difference of the arch index parameter on both sides; symmetry was preserved.

Table 14. Comparison of the arch index of operated and non-operated side in gamma group (n = 20) vs. control group (n = 20).

	Gamma Group	Control Group	p
AI operated side	25.42 ± 5.10	27.52 ± 3.74	0.15
AI opposite side	27.21 ± 4.94	27.76 ± 4.05	0.70

Values are expressed as mean ± standard deviation.

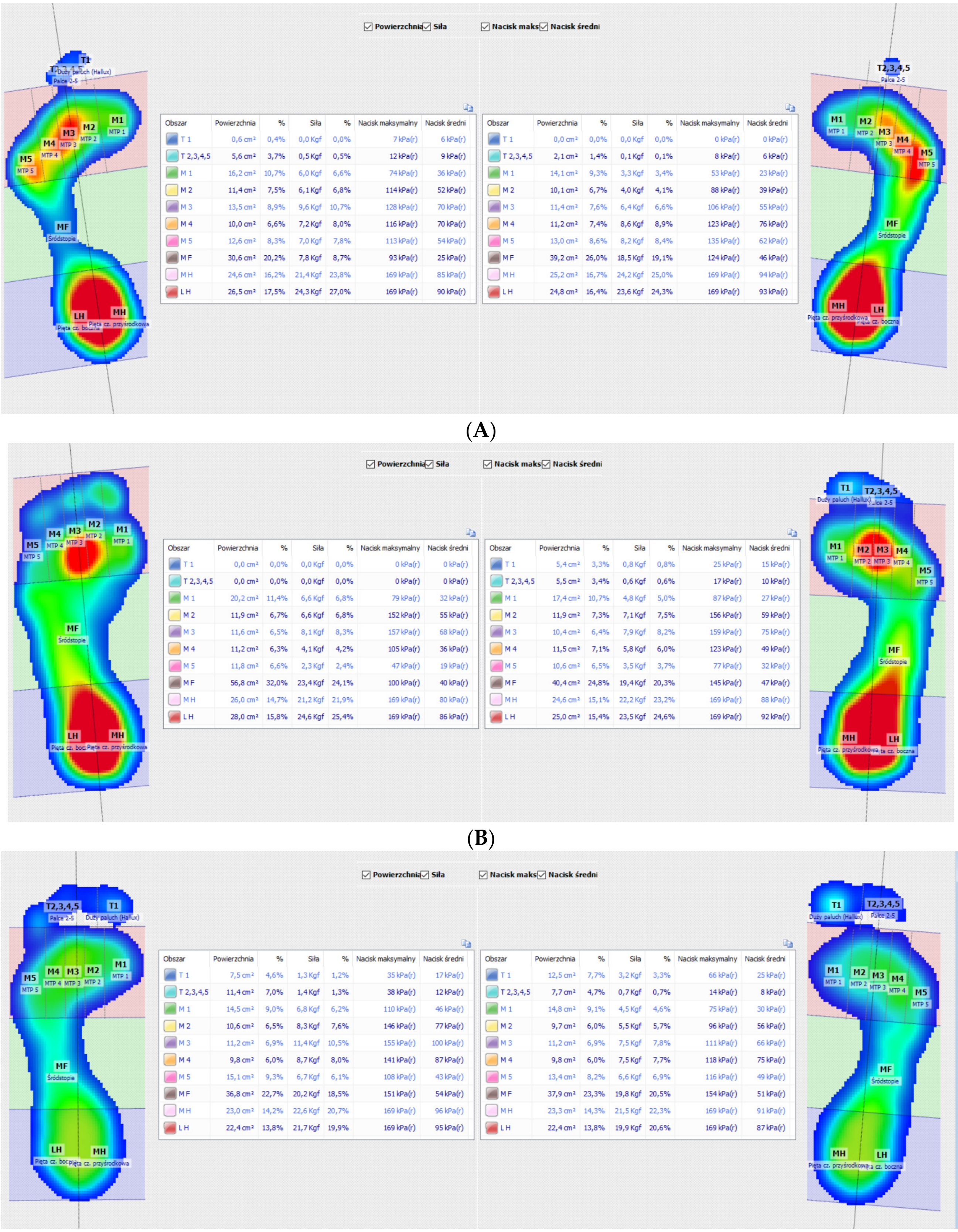

(**A**)

Obszar	Powierzchnia	%	Siła	%	Nacisk maksymalny	Nacisk średni
T 1	0,6 cm²	0,4%	0,0 Kgf	0,0%	7 kPa(r)	6 kPa(r)
T 2,3,4,5	5,6 cm²	3,7%	0,5 Kgf	0,5%	12 kPa(r)	9 kPa(r)
M 1	16,2 cm²	10,7%	6,0 Kgf	6,6%	74 kPa(r)	36 kPa(r)
M 2	11,4 cm²	7,5%	6,1 Kgf	6,8%	114 kPa(r)	52 kPa(r)
M 3	13,5 cm²	8,9%	9,6 Kgf	10,7%	128 kPa(r)	70 kPa(r)
M 4	10,0 cm²	6,6%	7,2 Kgf	8,0%	116 kPa(r)	70 kPa(r)
M 5	12,6 cm²	8,3%	7,0 Kgf	7,8%	113 kPa(r)	54 kPa(r)
M F	30,6 cm²	20,2%	7,8 Kgf	8,7%	93 kPa(r)	25 kPa(r)
M H	24,6 cm²	16,2%	21,4 Kgf	23,8%	169 kPa(r)	85 kPa(r)
L H	26,5 cm²	17,5%	24,3 Kgf	27,0%	169 kPa(r)	90 kPa(r)

Obszar	Powierzchnia	%	Siła	%	Nacisk maksymalny	Nacisk średni
T 1	0,0 cm²	0,0%	0,0 Kgf	0,0%	0 kPa(r)	0 kPa(r)
T 2,3,4,5	2,1 cm²	1,4%	0,1 Kgf	0,1%	8 kPa(r)	6 kPa(r)
M 1	14,1 cm²	9,3%	3,3 Kgf	3,4%	53 kPa(r)	23 kPa(r)
M 2	10,1 cm²	6,7%	4,0 Kgf	4,1%	88 kPa(r)	39 kPa(r)
M 3	11,4 cm²	7,6%	6,4 Kgf	6,6%	106 kPa(r)	55 kPa(r)
M 4	11,2 cm²	7,4%	8,6 Kgf	8,9%	123 kPa(r)	76 kPa(r)
M 5	13,0 cm²	8,6%	8,2 Kgf	8,4%	135 kPa(r)	62 kPa(r)
M F	39,2 cm²	26,0%	18,5 Kgf	19,1%	124 kPa(r)	46 kPa(r)
M H	25,2 cm²	16,7%	24,2 Kgf	25,0%	169 kPa(r)	94 kPa(r)
L H	24,8 cm²	16,4%	23,6 Kgf	24,3%	169 kPa(r)	93 kPa(r)

(**B**)

Obszar	Powierzchnia	%	Siła	%	Nacisk maksymalny	Nacisk średni
T 1	0,0 cm²	0,0%	0,0 Kgf	0,0%	0 kPa(r)	0 kPa(r)
T 2,3,4,5	0,0 cm²	0,0%	0,0 Kgf	0,0%	0 kPa(r)	0 kPa(r)
M 1	20,2 cm²	11,4%	6,6 Kgf	6,8%	79 kPa(r)	32 kPa(r)
M 2	11,9 cm²	6,7%	6,6 Kgf	6,8%	152 kPa(r)	55 kPa(r)
M 3	11,6 cm²	6,5%	8,1 Kgf	8,3%	157 kPa(r)	68 kPa(r)
M 4	11,2 cm²	6,3%	4,1 Kgf	4,2%	105 kPa(r)	36 kPa(r)
M 5	11,8 cm²	6,6%	2,3 Kgf	2,4%	47 kPa(r)	19 kPa(r)
M F	56,8 cm²	32,0%	23,4 Kgf	24,1%	100 kPa(r)	40 kPa(r)
M H	26,0 cm²	14,7%	21,2 Kgf	21,9%	169 kPa(r)	80 kPa(r)
L H	28,0 cm²	15,8%	24,6 Kgf	25,4%	169 kPa(r)	86 kPa(r)

Obszar	Powierzchnia	%	Siła	%	Nacisk maksymalny	Nacisk średni
T 1	5,4 cm²	3,3%	0,8 Kgf	0,8%	25 kPa(r)	15 kPa(r)
T 2,3,4,5	5,5 cm²	3,4%	0,6 Kgf	0,6%	17 kPa(r)	10 kPa(r)
M 1	17,4 cm²	10,7%	4,8 Kgf	5,0%	87 kPa(r)	27 kPa(r)
M 2	11,9 cm²	7,3%	7,1 Kgf	7,5%	156 kPa(r)	59 kPa(r)
M 3	10,4 cm²	6,4%	7,9 Kgf	8,2%	159 kPa(r)	75 kPa(r)
M 4	11,5 cm²	7,1%	5,8 Kgf	6,0%	123 kPa(r)	49 kPa(r)
M 5	10,6 cm²	6,5%	3,5 Kgf	3,7%	77 kPa(r)	32 kPa(r)
M F	40,4 cm²	24,8%	19,4 Kgf	20,3%	145 kPa(r)	47 kPa(r)
M H	24,6 cm²	15,1%	22,2 Kgf	23,2%	169 kPa(r)	88 kPa(r)
L H	25,0 cm²	15,4%	23,5 Kgf	24,6%	169 kPa(r)	92 kPa(r)

(**C**)

Obszar	Powierzchnia	%	Siła	%	Nacisk maksymalny	Nacisk średni
T 1	7,5 cm²	4,6%	1,3 Kgf	1,2%	35 kPa(r)	17 kPa(r)
T 2,3,4,5	11,4 cm²	7,0%	1,4 Kgf	1,3%	38 kPa(r)	12 kPa(r)
M 1	14,5 cm²	9,0%	6,8 Kgf	6,2%	110 kPa(r)	46 kPa(r)
M 2	10,6 cm²	6,5%	8,3 Kgf	7,6%	146 kPa(r)	77 kPa(r)
M 3	11,2 cm²	6,9%	11,4 Kgf	10,5%	155 kPa(r)	100 kPa(r)
M 4	9,8 cm²	6,0%	8,7 Kgf	8,0%	141 kPa(r)	87 kPa(r)
M 5	15,1 cm²	9,3%	6,7 Kgf	6,1%	108 kPa(r)	43 kPa(r)
M F	36,8 cm²	22,7%	20,2 Kgf	18,5%	151 kPa(r)	54 kPa(r)
M H	23,0 cm²	14,2%	22,6 Kgf	20,7%	169 kPa(r)	96 kPa(r)
L H	22,4 cm²	13,8%	21,7 Kgf	19,9%	169 kPa(r)	95 kPa(r)

Obszar	Powierzchnia	%	Siła	%	Nacisk maksymalny	Nacisk średni
T 1	12,5 cm²	7,7%	3,2 Kgf	3,3%	66 kPa(r)	25 kPa(r)
T 2,3,4,5	7,7 cm²	4,7%	0,7 Kgf	0,7%	14 kPa(r)	8 kPa(r)
M 1	14,8 cm²	9,1%	4,5 Kgf	4,6%	75 kPa(r)	30 kPa(r)
M 2	9,7 cm²	6,0%	5,5 Kgf	5,7%	96 kPa(r)	56 kPa(r)
M 3	11,2 cm²	6,9%	7,5 Kgf	7,8%	111 kPa(r)	66 kPa(r)
M 4	9,8 cm²	6,0%	7,5 Kgf	7,7%	118 kPa(r)	75 kPa(r)
M 5	13,4 cm²	8,2%	6,6 Kgf	6,9%	116 kPa(r)	49 kPa(r)
M F	37,9 cm²	23,3%	19,8 Kgf	20,5%	154 kPa(r)	51 kPa(r)
M H	23,3 cm²	14,3%	21,5 Kgf	22,3%	169 kPa(r)	91 kPa(r)
L H	22,4 cm²	13,8%	19,9 Kgf	20,6%	169 kPa(r)	87 kPa(r)

Figure 1. Graphic representation of the plantar pressure distribution after stabilization of the pertrochanteric fracture with a DHS (**A**) and gamma nail (**B**) and in control group (**C**).

3.3. Radiographic Analysis

Based on X-ray images, bone union was found in all 40 cases. Table 15 shows the comparison of the radiological parameters between the DHS and gamma groups. The mean values of the minimum distance between the tip of the neck screw and the articular surface of the femoral head were greater in the DHS group than The gamma group (14.75 vs. 10.27). In the other tested parameters, the obtained results do not indicate any significant difference in the distribution between both groups.

Table 15. Comparison of parameters related to selected parameters based on the X-rays in DHS group (n = 20) and gamma group (n = 20).

	DHS Group	Gamma Group	p
NSA—non-operated side (degrees)	131.90 ± 2.57	130.90 ± 2.00	0.18
NSA—operated side (degrees)	133.60 ± 3.38	131.75 ± 2.67	0.06
The minimum distance between the tip of the neck screw and the articular surface of the femoral head (millimeters)	14.75 ± 5.63	10.27 ± 3.45	0.00 *

Values are expressed as mean ± standard deviation. * $p < 0.05$.

The position of the neck screw in relation to the axis of the femoral neck:

1. DHS group: in 19 patients the screw was located on the axis or below, in 1 patient the screw was located above the axis.
2. Gamma group: in 18 patients the screw was located on the axis or below, in 2 patients the screw was located above the axis.

The axis of the intramedullary nail in relation to the axis of the femur: varus position—4 subjects; axial position—15 subjects; valgus position—1 subject.

The difference in the height of the trochanter position is smaller/shortened length of the operated limb by >1 cm: in DHS group—1 subjects, gamma group: 3 subjects.

4. Discussion

Human symmetry largely depends on the lack of posttraumatic lesions. The most relevant finding resulting from this paper is the lack of symmetry disorders observed in the older patients post status surgical restoration of the native anatomical relationships within the proximal end of the femur, regardless of the method used. Analysis of the literature shows a continuously rising number of osteoporotic fractures as a consequence of the ever-growing trend of the aging population. Increasing age and female gender are the main factors associated with osteoporosis and fractures [4,21]. This is also evidenced by the data obtained from our research—in the study group, there were 33 women and 7 men, and the oldest person was 99 years old. With age, a human's health undergoes a gradual deterioration. The age-related involution changes are usually accompanied by diseases including those related to the nervous system, cardiovascular system and locomotor system [21]. Based on the literature review, over the first year after the PFs injury, the mortality rate is up to 30%. A broad analysis of studies shows that during the COVID-19 pandemic, among patients who were surgically treated for proximal femur fractures or hip fractures, the total mortality rate was 30.4% for COVID-19 positive patients and 10.3% for patients without coronavirus [22–26]. Therefore, it can be explained by a small number of people in the study group. According to the previous authors' publication, the number of patients attending subsequent follow-up visits after surgical treatment of PFs was systematically decreasing [27].

The present study revealed no significant difference between functional outcomes assessed by the Harris Hip Score in both groups, the DHS and gamma groups, at 9-month follow-up. As reported by the authors' previous research, there were also no differences observed between both study groups at 3-month and 6-month follow-up. Studies by Chang et al. [28] confirmed the lack of a significant difference between the operated groups. In this case the follow-up duration ranged from 3 to 19 months (mean follow-up duration = 10.06 months). Better results than ours were obtained by Selim et al. and Catania et al., who examined patients who underwent DHS + TSP fixation and gamma nail fixation during 6-month follow-up, 83.32 $\pm$ 9.73 (mean, SD) in the case of DHS + TSP and 84.25 $\pm$ 8.19 (mean, SD) in the case of gamma nail [10,11].

Analysis of the plantar pressure distribution with a pedobarograph is a non-invasive method used to evaluate various types of structural and functional disorders of the musculoskeletal system, including the symmetry of lower limbs after surgical treatment. It is not only an important diagnostic tool but also has a prognostic element. It enables the preparation and monitoring of the treatment applied, including physiotherapy.

It should be emphasized that among the factors conducive to the formation of asymmetry in the pressure distribution in patients after PFs, except for morphological conditions, there are also biomechanical properties of the hip joint. The bearing function of the hip joint is constantly modified as a result of the changes in the level of pressures' concentration in its range. The abnormal distribution of loads create favorable conditions for a quick development of post-injury degenerative changes. According to T. Myers, fascial connections between muscular structures along the axis of the limbs and the torso form chains of the so-called anatomy trains. Disorders within these myofascial structures manifest with pain and limited mobility, as well as changes in the mobility of other tissues far from the location of injury or surgical intervention [29]. The mechanics of the iliofemoral articulation and the whole bone–muscle chain of the lower limb, including the axial skeleton, are disturbed by the amortization of excessive static and dynamic stresses. Pedobarographic study of plantar pressure distribution demonstrates how surgical treatment after PFs using a DHS screw plate and intramedullary gamma nail maintains the symmetry of foot loading.

The pedobarographic analysis was carried out in a static mode, in order to ensure the maximum safety of the participants. Some of the respondents used assistive devices while walking—a walker or cane. Dynamic analysis requires greater mobility and stability while walking. The epidemiological safety is also worth mentioning. The pedobarographic platform is easy to disinfect and the risk of fungal contamination is kept to a minimum, unlike testing with an insole-based system and reusable footwear. Since the SARS-CoV-2 infection outbreak in Wuhan, China, in December 2019, it is crucial to ensure safety in order to reduce the risk of contamination [18]. However, this problem has always existed because the frequency of fungal infections in the elderly population remains very high. Hence, the great ethical doubts of the authors regarding the use of reusable insoles worn by many people, usually sports shoes used for diagnostics. In our opinion, such equipment should be either disposable or fully disinfectable.

The present study revealed no significant difference in the entire foot loading of the operated and non-operated sides in both study groups. This is a good result showing that the anatomy of the fractured limb was surgically reconstructed. In both study groups the opposite side is more loaded than the operated side (59.21 vs. 58.74, respectively, in the DHS group and 57.45 vs. 56.58, respectively, in the gamma group). There is a tendency for a greater load on the operated side, but the difference in the loading remains statistically insignificant; therefore, it is assumed that the symmetry under the entire foot is maintained. The comparison of the pressure distribution under the entire foot between the DHS and gamma groups also showed no significant difference both in the operated and non-operated lower limbs. Therefore, it can be assumed that the type of anastomosis used does not significantly affect the symmetry of foot loading in the study group. Detailed comparison of the plantar pressure distribution in the masked regions of the foot showed no significant difference in loading in both study groups. It should be remembered that the test was carried out under static conditions. In order to fully assess the symmetry of foot loading, it should be supplemented with dynamic measurements while walking. We presume that in the case of walking, the variability of the foot pressure would be significant. Posttraumatic degenerative changes in the iliofemoral articulation contribute to foot loading asymmetry. All articulations of the lower limb work in constrained positions by reason of looking for a painless amplitude of movements in the iliofemoral articulation.

The author of this work obtained different results in a previous study. He demonstrated that in people after PFs, an asymmetry of loads occurs in the T1, T2–5, MH and LH zones [30]. The discrepancy in results may be due to a longer follow-up period of 2–4 (mean 2.80) years after PFs' injury. In such a long period, it is likely to develop severe posttraumatic degenerative changes, which affect the symmetry of foot loading.

There were significant differences in plantar pressure distribution between the study group and the control group. This applies to both study groups. The image of the pedobarographic examination shows that despite surgical restoration of the correct mutual anatomical relations, complete union and 9-month rehabilitation treatment, the full symmetry, characteristic of the control group, was not restored while standing. This is important because there is no significant difference between both study groups (DHS and gamma) across the entire foot pressure distribution (operated side: 58.74 DHS v. 56.58 gamma, opposite side: 59.21 DHS v. 57.45 gamma). Thus, the pedobarographic examination shows that the fracture left permanent defects in the function of the musculoskeletal system. This is consistent with the results based on the Harris Hip Score questionnaire.

No significant differences were found in the arch index between subjects operated with both analyzed methods. There were also no differences between each of these groups individually and the control group. Responsibility for the arch index lies with the osteoarticular and ligamentous-muscular systems. The lack of differences indicates that there was no significant power decline in the muscle structures responsible for the arch index in any of the analyzed cases. This, therefore, proves the need for proper and early rehabilitation treatment.

The initial stage of rehabilitation began with the patient's upright position (sitting) on the first day after the surgery. The patients were taught the following exercises: isometric exercise of quadriceps and gluteal muscles, anticoagulant exercises and respiratory exercises. On the second postoperative day, the following exercises, tailored to the individual capabilities of the patient, were added: active slow exercises of lower extremity, gait reeducation and assisted walking with weight-bearing tolerance using a Zimmer frame. These exercises were continued throughout the patient's stay in the hospital. After discharge, patients participated in a home rehabilitation therapy after PFs.

Analysis of the problem of functional results after the treatment of pertrochanteric fractures in the elderly shows that the existing compensation mechanisms cannot be ignored. Older people use more neural networks within the brain to perform a simple, and even more complex, motor task. Within this network, as they get older, they are more likely to activate more regions [31]. The reason for this may be compensation mechanisms consisting of the reorganization and redistribution of the transmitted signals within the aging neural network. Research by Ward and Frackowiak shows that compensatory processes can help some people maintain their performance levels. However, these are not simple linear relationships. The anatomical structures involved in the process of motor compensation are mainly the ventral premotor cortex (Brodmann area 44), intraparietal sulcus, deep part of anterior central sulcus, caudal dorsal premotor cortex, caudal cingulate sulcus and some parts of the insula, frontal operculum and cerebellar vermis [32]. The described phenomenon applies not only to humans but is also commonly known in nature. The observations of Romano at al. regarding neuro-compensatory behavior in locusts seem very interesting here. Older individuals undertake neuromotor activities earlier. This may be due to compensatory behavior based on a slower muscle response, which may take a longer time to complete. Knowledge of these mechanisms can be used to alleviate motor disorders in elderly patients [33]. In our opinion, in each case of a trochanteric fracture, due to the degree of primary destruction of the musculoskeletal system, the organism's compensatory reaction had to be similar. The results of pedobarographic research indicate that the image of full symmetry was not obtained, so the body of an elderly person had to adapt to the new functional anatomy of the musculoskeletal system. A compensatory contribution of the central nervous system as a whole was indispensable.

Based on x-ray images, bone union was achieved in all the cases in the entire study group treated with the DHS method and gamma nail. Full bone union is the key factor enabling symmetry because it is based on the correct surgical reconstruction of the axis of the operated lower limb. Regarding the neck-shaft angle, the obtained values indicate the presence of symmetry in the operated and non-operated lower limbs. The results confirm the correct restoration of the lower limb axis, which was also evidenced in our earlier studies [27].

The significant difference between the DHS group and gamma group was maintained in the parameter concerning the minimum distance between the tip of the neck screw and the articular surface of the femoral head. In each case, the cervical screw did not penetrate into the articular cartilage or the joint cavity, which was clinically significant, as it rendered an additional anastomosis removal surgery unnecessary.

The position of the neck screw in relation to the axis of the femoral neck was another parameter that we examined [34]. We found the screw in the majority of cases located on the axis or below the axis of the femoral neck (in 37 cases). The obtained result is compliant with the applicable standards and with the results obtained during the study covering a larger group of patients during the 6-month follow-up [24]. In three cases, the screw was placed above the axis because of the previous microanatomy changes in the neck of the femoral bone. With regard to intramedullary nails, we additionally checked their axial insertion into the femoral bone. Most of the subjects (15 subjects) obtained axial insertion, which is also confirmed by the results of other researchers [35].

Shortening of the operated limb is one of the key parameters of X-ray assessment in the context of symmetry evaluation. The commonly used >1 cm of the limb length discrepancy we found to be significant and included in our result. After careful examination we noticed four cases of such a distortion: one patient in the DHS group and three patients treated with gamma nail. This may be due to the fact that the gamma nails were used to stabilize more unstable, multi-fragmented fractures; hence, more complications are possible.

To sum up the radiographic analysis, good treatment results were obtained in both study groups. Despite the fact that gamma nails are commonly used for unstable fractures requiring more technical skills from the operator, they seem to be a better choice.

This study has potential limitations. The first focus on the insufficient sample size for good statistical measurements. The results presented herein were observed in a cohort of only 40 patients after PFs. Additionally the short follow-up period does not allow for a long-term evaluation of the results. Moreover, the occurrence of foot disorders such as hallux valgus, calluses and soft tissue pathology may distort the test result. Comparative studies also come under an inherent risk of bias. The lack of comparison of complications after surgery is another disadvantage. However, we believe that in this research we have demonstrated the practical use of pedobarography in the quantitative evaluation of plantar pressure distribution in the diagnosis of the symmetry in foot loading after the surgical treatment of pertrochanteric fractures.

5. Conclusions

1. In all the examined subjects, despite the extent of the injury, compensatory mechanisms were found, for which the central nervous system is probably responsible. This seems to lead to a functional symmetry between the outcomes of the surgical treatment of PFs in people treated with a dynamic hip screw and an intramedullary gamma nail.
2. Biomechanical scoring of plantar pressure distribution in all regions as well as the arch index shows symmetry between the DHS group and gamma group.
3. In order to significantly improve the results of PFs' treatment, it is necessary to take into account the compensatory mechanisms and the results of not only radiological but biomechanical analyses of operated patients.

Author Contributions: Conceptualization, J.L. and K.G.; methodology, J.L. and K.G.; software, J.L. and K.G.; validation, J.L. and K.G.; formal analysis, J.L. and K.G.; investigation, J.L. and K.G.; resources, J.L. and K.G.; data curation, J.L. and K.G.; writing—original draft preparation, J.L. and K.G.; writing—review and editing, J.L. and K.G.; visualization, J.L. and K.G.; supervision, J.L. All authors have read and agreed to the published version of the manuscript.

Funding: This research received no external funding.

Institutional Review Board Statement: Informed consent was obtained from all subjects involved in the study, as required by Ethical Committee.

Informed Consent Statement: Informed consent was obtained from all subjects involved in the study.

Data Availability Statement: The data presented in this study are available on request from the corresponding authors.

Conflicts of Interest: The authors declare no conflict of interest.

References

1. Mandelbrot, B.B. *The Fractal Geometry of Nature*; W.H. FreemanSan: San Francisco, CA, USA, 1983; ISBN 978-0-7167-1186-5.
2. Kar, M.; Muluk, N.B.; Bafaqeeh, S.A.; Cingi, C. Is it possible to define the ideal lips? *Acta Otorhinolaryngol. Ital.* **2018**, *38*, 67–72. [CrossRef] [PubMed]
3. Hope, D.; Bates, T.C.; Dykiert, D.; Der, G.; Deary, I.J. Bodily symmetry increases across human childhood. *Early Hum. Dev.* **2013**, *89*, 531–535. [CrossRef] [PubMed]
4. Aspray, T.J.; Hill, T.R. Osteoporosis and the Ageing Skeleton. *Subcell. Biochem.* **2019**, *91*, 453–476. [CrossRef] [PubMed]
5. Borgström, F.; Karlsson, L.; Ortsäter, G.; Norton, N.; Halbout, P.; Cooper, C.; Lorentzon, M.; McCloskey, E.V.; Harvey, N.C.; Javaid, M.; et al. International Osteoporosis Foundation. Fragility fractures in Europe: Burden, management and opportunities. *Arch. Osteoporos.* **2020**, *15*, 59. [CrossRef] [PubMed]
6. Ucurum, S.G.; Altas, E.U.; Kaya, D.O. Comparison of the spinal characteristics, postural stability and quality of life in women with and without osteoporosis. *J. Orthop. Sci.* **2020**, *25*, 960–965. [CrossRef]
7. Osoba, M.Y.; Rao, A.K.; Agrawal, S.K.; Lalwani, A.K. Balance and gait in the elderly: A contemporary review. *Laryngosc. Investig. Otolaryngol.* **2019**, *4*, 143–153. [CrossRef]
8. Anandasivam, N.S.; Russo, G.S.; Fischer, J.M.; Samuel, A.; Ondeck, N.T.; Swallow, M.S.; Chung, S.H.; Bohl, D.D.; Grauer, J.N. Analysis of Bony and Internal Organ Injuries Associated with 26,357 Adult Femoral Shaft Fractures and Their Impact on Mortality. *Orthopedics* **2017**, *40*, e506–e512. [CrossRef]
9. Saul, D.; Riekenberg, J.; Ammon, J.C.; Hoffmann, D.B.; Sehmisch, S. Hip Fractures: Therapy, Timing, and Complication Spectrum. *Orthop. Surg.* **2019**, *11*, 994–1002. [CrossRef]
10. Selim, A.; Ponugoti, N.; Zain Naqvi, A.; Magill, H. Cephalo-medullary nailing versus dynamic hip screw with trochanteric stabilisation plate for the treatment of unstable per-trochanteric hip fractures: A meta-analysis. *J. Orthop. Surg. Res.* **2021**, *16*, 1–9. [CrossRef]
11. Catania, P.; Passaretti, D.; Montemurro, G.; Ripanti, S.; Carbone, S.; Candela, V.; Carnovale, M.; Gumina, S.; Pallotta, F. Intramedullary nailing for pertrochanteric fractures of proximal femur: A consecutive series of 323 patients treated with two devices. *J. Orthop. Surg. Res.* **2019**, *18*, 449. [CrossRef]
12. Kempf, I.; Grosse, A.; Taglang, G.; Favreul, E. Gamma nail in the treatment of closed trochanteric fractures. Results and indications of 121 cases. *Orthop. Traumatol. Surg. Res.* **2014**, *100*, 75–83. [CrossRef] [PubMed]
13. Lorkowski, J.; Gawronska, K. Pedobarography in Physiotherapy: A Narrative Review on Current Knowledge. *Adv Exp Med Biol.* **2021**, *1375*, 13–22. [CrossRef]
14. Harris, W.H. Traumatic Arthritis of the Hip after Dislocation and Acetabular Fractures: Treatment by Mold Arthroplasty an end-result study using a new method of results evaluation. *J. Bone Jt. Surg. Am.* **1969**, *51*, 737–755. [CrossRef]
15. Babhulkar, S. Unstable trochanteric fractures: Issues and avoiding pitfalls. *Injury* **2017**, *48*, 803–818. [CrossRef] [PubMed]
16. Hopp, S.; Wirbel, R.; Ojodu, I.; Pizanis, A.; Pohlemann, T.; Fleischer, J. Does the implant make the difference? Prospective comparison of two different proximal femur nails. *Acta Orthop. Belg.* **2016**, *82*, 319–331.
17. Zhang, H.; Zeng, X.; Zhang, N.; Zeng, D.; Xu, P.; Zhang, L.; Chen, D.; Yu, W.; Zhang, X. INTERTAN nail versus proximal femoral nail antirotation-Asia for intertrochanteric femur fractures in elderly patients with primary osteoporosis. *J. Int. Med. Res.* **2017**, *45*, 1297–1309. [CrossRef]
18. Lorkowski, J.; Gawronska, K.; Pokorski, M. Pedobarography: A Review on Methods and Practical Use in Foot Disorders. *Appl. Sci.* **2021**, *11*, 11020. [CrossRef]
19. Cavanagh, P.R.; Rodgers, M.M. The arch index: A useful measure from footprints. *J. Biomech.* **1987**, *20*, 547–551. [CrossRef]
20. Cavanagh, P.R.; Rodgers, M.M.; Iiboshi, A. Pressure distribution under symptom-free feet during barefoot standing. *Foot Ankle.* **1987**, *7*, 262–276. [CrossRef]
21. Khow, K.S.F.; Visvanathan, R. Falls in the Aging Population. *Clin. Geriatr. Med.* **2017**, *33*, 357–368. [CrossRef]

22. Muñoz Vives, J.M.; Jornet-Gibert, M.; Cámara-Cabrera, J.; Esteban, P.L.; Brunet, L.; Delgado-Flores, L.; Camacho-Carrasco, P.; Torner, P. Mortality Rates of Patients with Proximal Femoral Fracture in a Worldwide Pandemic: Preliminary Results of the Spanish HIP-COVID Observational Study. *J. Bone Jt. Surg. Am.* **2020**, *102*, e69. [CrossRef] [PubMed]
23. Hadfield, J.N.; Gray, A.C. The Evolving COVID-19 Effect on Hip Fracture Patients. *Injury* **2020**, *51*, 1411–1412. [CrossRef] [PubMed]
24. Dupley, L.; Oputa, T.J.; Bourne, J.T. North West COVID NOF Study Group. 30-day mortality for fractured neck of femur patients with concurrent COVID-19 infection [published online ahead of print, 4 September 2020]. *Eur. J. Orthop. Surg. Traumatol.* **2021**, *31*, 341–347. [CrossRef] [PubMed]
25. Kumar, J.V.; Lal, H.; Kumar, P.M.; Vaishya, R. Fracture management during COVID-19 pandemic: A systematic review. *J. Clin. Orthop. Trauma.* **2020**, *11* (Suppl. S4), 431–441. [CrossRef] [PubMed]
26. Maniscalco, P.; Poggiali, E.; Quattrini, F.; Ciatti, C.; Magnacavallo, A.; Vercelli, A.; Domenichini, M.; Vaienti, E.; Pogliacomi, F.; Ceccarelli, F. Proximal femur fractures in COVID-19 emergency: The experience of two Orthopedics and Traumatology Departments in the first eight weeks of the Italian epidemic. *Acta Biomed.* **2020**, *91*, 89–96. [CrossRef]
27. Gawronska, K.; Lorkowski, J. Functional Symmetry after Surgical Treatment of Pertrochanteric Fractures in the Elderly. *Symmetry* **2022**, *14*, 393. [CrossRef]
28. Cheng, Y.X.; Sheng, X. Optimal surgical methods to treat intertrochanteric fracture: A Bayesian network meta-analysis based on 36 randomized controlled trials. *J. Orthop. Surg. Res.* **2020**, *15*, 402. [CrossRef]
29. Myers, T.W. *Anatomy trains e-book: Myofascial Meridians for Manual and Movement Therapists*; Elsevier Health Sciences: London, UK, 2013.
30. Lorkowski, J.; Waldemar, H.Å.; Trybus, M.; Zarzycki, D. Underfoot pressure distribution in patients after surgical treatment of proximal end of femoral bone. *J. Orthop. Trauma Surg. Relat. Res.* **2009**, *4*, 3.
31. Mattay, V.S.; Fera, F.; Tessitore, A.; Hariri, A.R.; Das, S.; Callicott, J.H.; Weinberger, D.R. Neurophysiological correlates of age-related changes in human motor function. *Neurology* **2002**, *58*, 630–635. [CrossRef]
32. Ward, N.S.; Frackowiak, R.S. Age-related changes in the neural correlates of motor performance. *Brain* **2003**, *126*, 873–888. [CrossRef]
33. Romano, D.; Bloemberg, J.; Tannous, M.; Stefanini, C. Impact of Aging and Cognitive Mechanisms on High-Speed Motor Activation Patterns: Evidence from an Orthoptera-Robot Interaction. *IEEE Trans. Med. Robot. Bionics* **2020**, *2*, 292–296. [CrossRef]
34. Mao, W.; Ni, H.; Li, L.; He, Y.; Chen, X.; Tang, H.; Dong, Y. Comparison of Baumgaertner and Chang reduction quality criteria for the assessment of trochanteric fractures. *Bone Jt. Res.* **2019**, *8*, 502–550. [CrossRef] [PubMed]
35. Tsai, S.W.; Lin, C.J.; Tzeng, Y.H.; Lin, C.C.; Huang, C.K.; Chang, M.C.; Chiang, C.C. Risk factors for cut-out failure of Gamma3 nails in treating unstable intertrochanteric fractures: An analysis of 176 patients. *J. Chin. Med. Assoc.* **2017**, *80*, 587–594. [CrossRef] [PubMed]